Electronic Supplementary Material (ESI) for Journal of Materials Chemistry A.


Supporting Information

# Fast and highly reversible switch of wettability through macroscopic shape change

Fatang Liu, Qinmin Pan*

(State Key Laboratory of Robotics and Systems, School of Chemistry and Chemical Engineering, Harbin Institute of Technology, Harbin 150001, P. R. China)

**Synthesis of superhydrophobic PVA-EG gel**

The PVA-EG gel was immersed in an *n*-hexane solution of methyl trichlorosilane (1.2%v/v) for 10 min and the resulting gel was dried at 60 °C for 20 min. The obtained PVA-EG gel showed contact angles of 153 ± 2° and ~0° for a water and a $CHCl_3$ droplet, respectively. Since trichloromethylsilane ($CH_3SiCl_3$) has a strong tendency to hydrolysis, [1-2] it easily formed a hierarchical structure on the PVA-based gels that contained considerable amount of water.

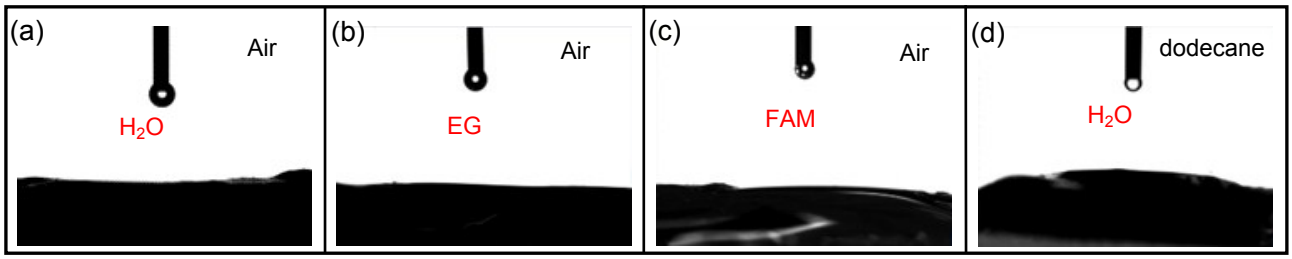


Fig. S1. Contact angles of the PVA-EG gel for a droplet of (a) water, (b) EG, (c) FAM and (d) water in *n*-dodecane.

The superamphiphilic PVA-EG gel was synthesized by filling ethylene glycol into PVA supramolecular structure through a solvent-exchange process.[3] In a typical experiment, aqueous PVA solution was firstly converted to PVA hydrogel by using borax as cross-linking agent. The obtained PVA hydrogel was then dipped in ethylene glycol, which allowed the water trapped in the PVA supramolecular structure to be replaced by ethylene glycol. The resulting PVA-EG gel had high affinity to both water and oils, since its surface showed almost zero contact angles to both water and oleophilic solvents like ethylene glycol and FAM (Fig. S1). The superamphiphobic copper meshes were fabricated by simply dipping copper meshes into an aqueous solution of $NaOH/K_2S_2O_8$[4] and subsequent modification with 1H,1H,2H,2H-perfluorodecyltriethoxysilane. They had needle-like hierarchical microstructures (Fig. S3a-b). The resulting meshes exhibited contact angles greater than 150° for water, ethylene glycol and FAM. Moreover, the mesh also showed under-oil superhydrophobicity when it was immersed in *n*-dodecane (Fig. S3c-g).

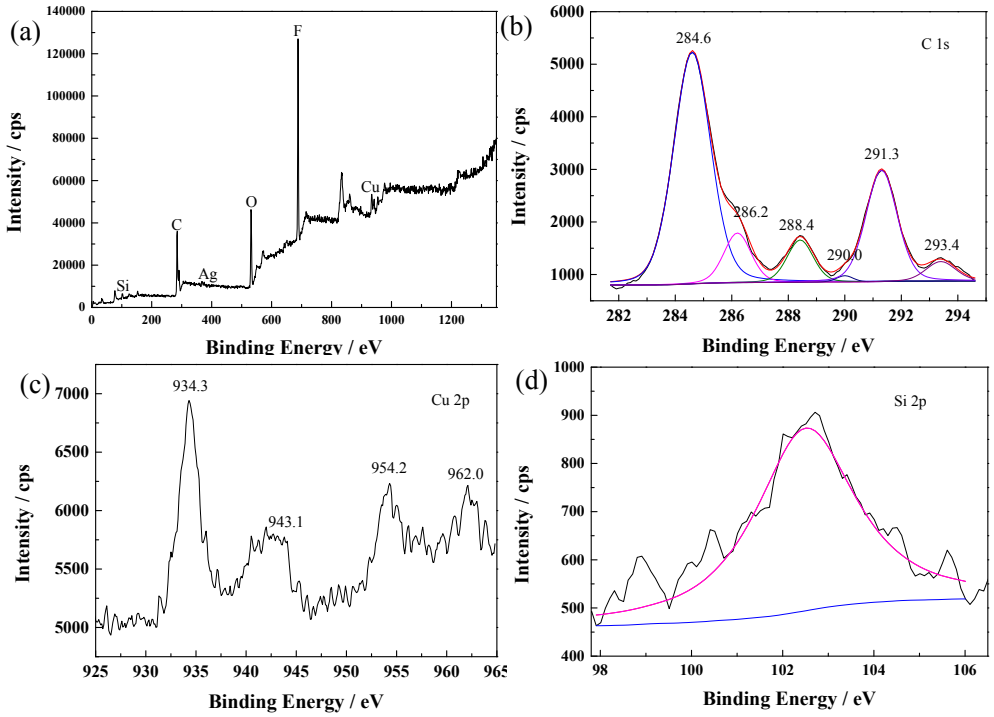


Fig. S2. XPS spectra of superhydrophobic copper mesh. (a) survey scan, (b) C 1s, (c) Cu 2p, (d) Si 2p.

The chemical composition of the superhydrophobic copper mesh was studied by XPS measurement (Fig. S2). The survey scan shows the elements of C, Si, Ag, O, F and Cu. In the C 1s spectra, the peaks at 284.6, 286.2 and 288.4 eV are assigned to C–C, C–O and C–O–Si, respectively.[5-6] The peaks at 290.0, 291.3 and 293.4 eV are ascribed to $-CH_2-\underline{C}F_2$, $-CF_2$ and $-CF_3$,[7-8] respectively, indicating that the copper mesh has been modified by 1H,1H,2H,2H-perfluorodecyltriethoxysilane. In the Cu 2p spectra, there are peaks at 934.3 and 954.2 eV and two shake-up lines at 943.1 and 962.0 eV, which confirms the existence of $Cu(OH)_2$ on the superhydrophobic copper mesh.[9] For the Si 2p spectra, the peak ascribed to Si-O of 1H,1H,2H,2H-perfluorodecyltriethoxysilane is located at 102.5 eV.[10]

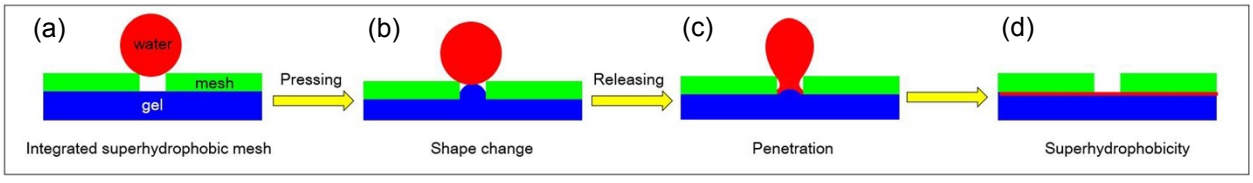


Fig. S3. Illustration schematics the mechanism of reversible wettability switch of the integrated superhydrophobic mesh.

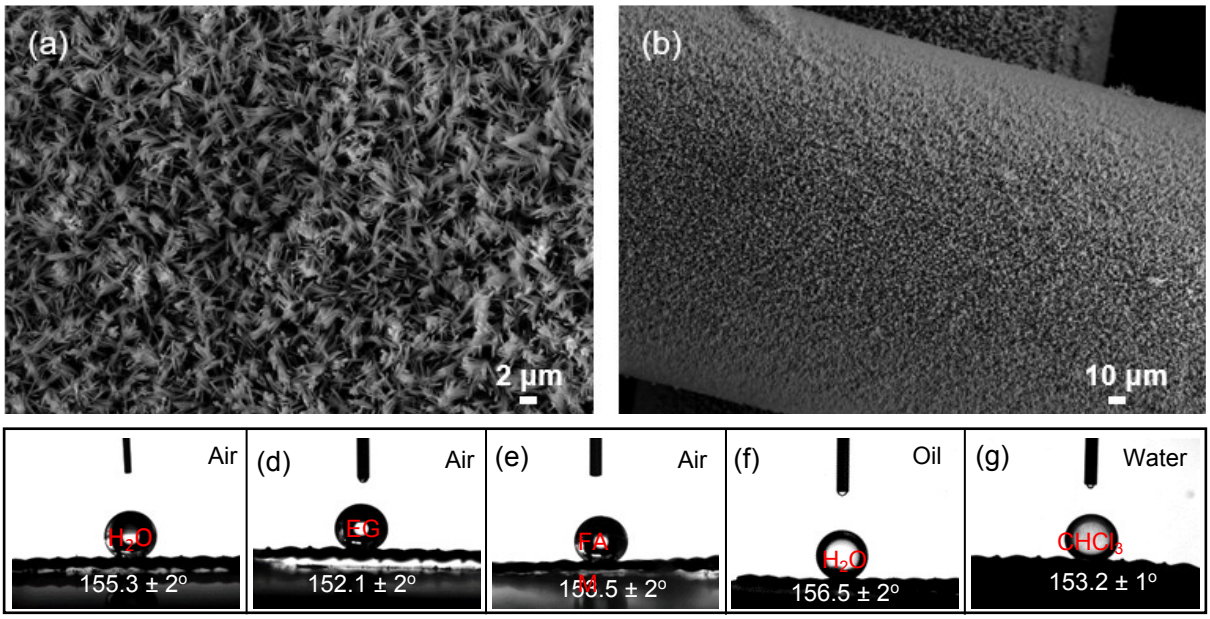


Fig. S4. (a and b) SEM images of the superhydrophobic copper mesh. Contact angles of the copper mesh for a droplet of (c) water, (d) EG, and (e) FAM. (f) Under-oil contact angle of the mesh for a water droplet, the mesh was immersed in *n*-dodecane. (g) Under-water contact angle of the mesh for a $CHCl_3$ droplet, the copper mesh without the treatment of 1H,1H,2H,2H-perfluorodecyltriethoxysilane was used.

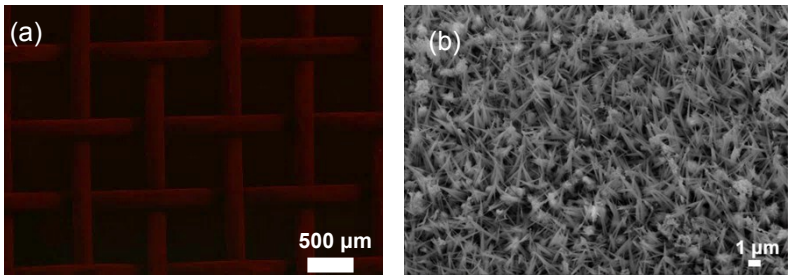


Fig. S5. (a) Fluorescent and (b) SEM image of the integrated PVA-EG/mesh after 60$^{th}$ switch for water droplets.

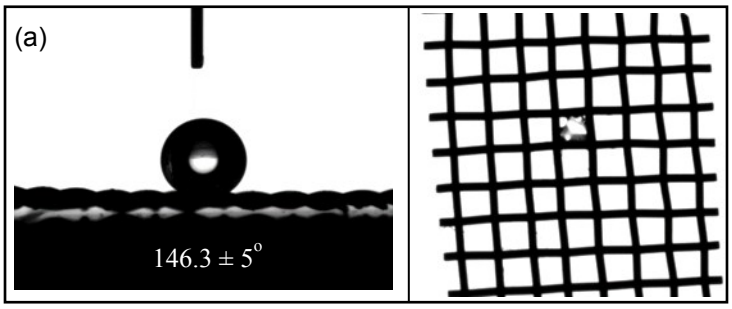

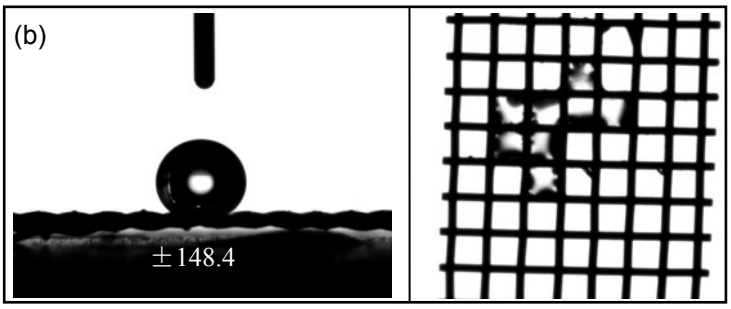


Fig. S6. Contact angles (left) and liquid films (right) formed on the PVA hygrogel/mesh after switch (a) water droplets for 6 cycles and (b) EG droplets for 4 cycles.

As shown in Fig. S6a and S6b, the integrated PVA hydrogel/mesh lost its superhydrophobicity after switch the water and EG droplets for 6 and 4 cycles, respectively. The failure is due to the formation of liquid films on the copper mesh (the right images).

Table S1. Comparison on the switch capability of typical special-wetting surfaces reported in literatures.

| Special-wetting surface | Stimuli | Switch wettability | Switch time | Switch cycle | Reference |
|---|---|---|---|---|---|
| Superhydrophobic cotton fabric | pH | Superhydrophilicity/superhydrophobicity | 55 s | 6 | 11 |
| ZnO-coated mesh | $H_2/O_2$ anneal | Superhydrophilicity/superhydrophobicity | 1.5 h | 10 | 12 |
| pH-Responsive Sponges | pH | Superhydrophilicity/superhydrophobicity | — | 10 | 13 |
| Graphene Foam | pH | Superhydrophilicity/superhydrophobicity | — | 10 | 14 |
| Janus mesh | — | Superhydrophilicity/superhydrophobicity | 5 s | — | 15 |
| $CO_2$-Responsive Nanofibrous Membranes | $CO_2$ | hydrophilicity/hydrophobicity | 300 s | 4 | 16 |
| ZnO superhydrophobic surfaces | UV | Superhydrophilicity/superhydrophobicity | 1 day | 5 | 17 |
| Superhydrophobic mesh | Electricity | Superhydrophilicity/superhydrophobicity | ⩾20 min | — | 18 |
| Polymer brush-functionalized surfaces | UV & pH | hydrophilicity/hydrophobicity | 20 min | 4 | 19 |
| Polymer superhydrophobic surfaces | Voltage | Superhydrophilicity/superhydrophobicity | — | 10 | 20 |
| Molecular brush-grafted surface | Temperature | hydrophilicity/hydrophobicity | — | 4 | 21 |
| PNIPAAm/HFMS surface | Temperature | Underwater Superoleophobicity/superoleophilicity | 1000 s | 5 | 22 |

| | | | | | |
|---|---|---|---|---|---|
| Integrated superhydrophobic mesh | Pressure | Superhydrophilicity/superhydrophobicity | < 2 s | 500 | Our work |

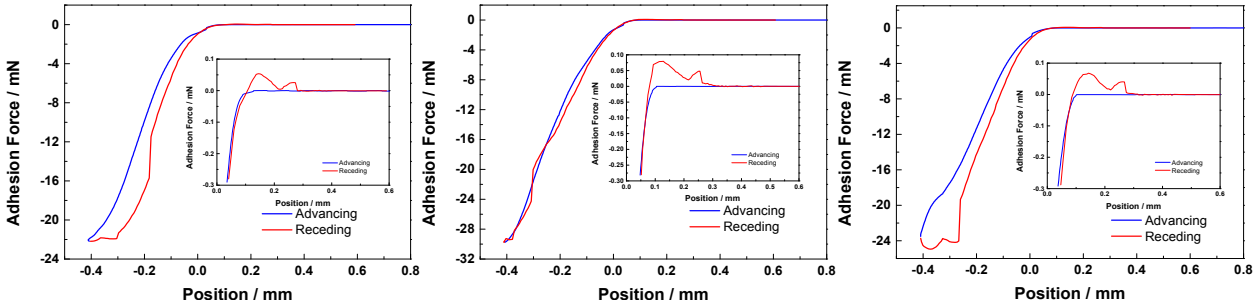


Fig. S7. Adhesion forces between the superhydrophobic copper mesh and the PVA-FAM gels after the 1st switch of (a) water, (b) EG and (c) FAM droplets.

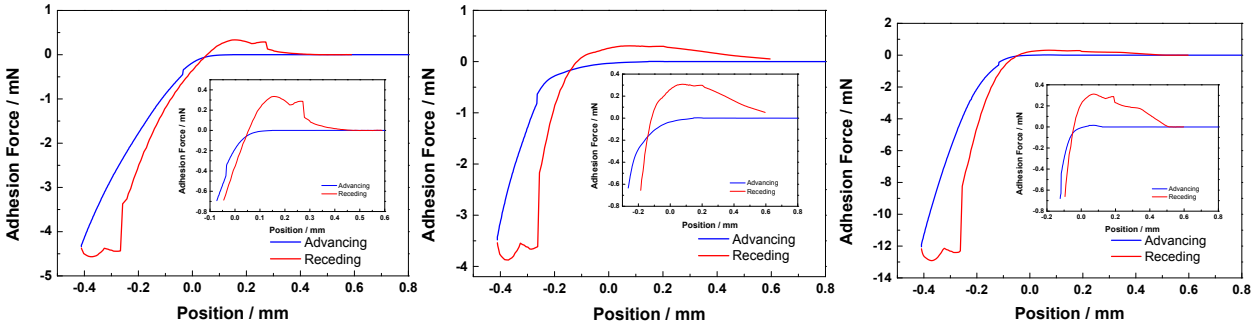


Fig. S8. Adhesion forces between the PVA-EG gels and the superhydrophobic copper mesh after switch (a) water droplets for 60 cycles, (b) EG droplets for 170 cycles and (c) FAM droplets for 190 cycles.

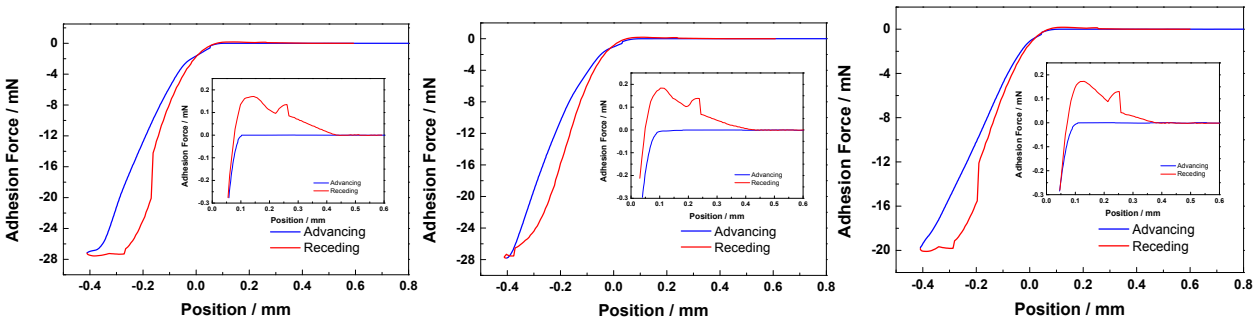


Fig. S9. Adhesion forces between the PVA-FAM gels and the superhydrophobic copper mesh after switch (a) water droplets for 500 cycles, (b) EG droplets for 280 cycles and (c) FAM droplets for 310 cycles.

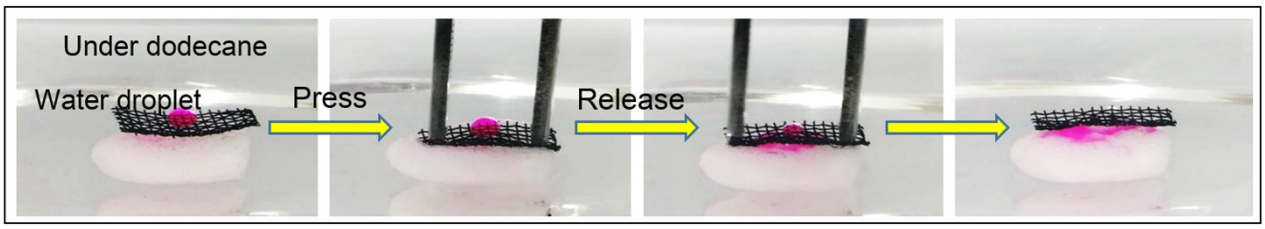

Fig. S10. Optical images record the wettability switch of a water droplet on the integrated PVA-EG/mesh immersed in *n*-dodecane for 4 d.

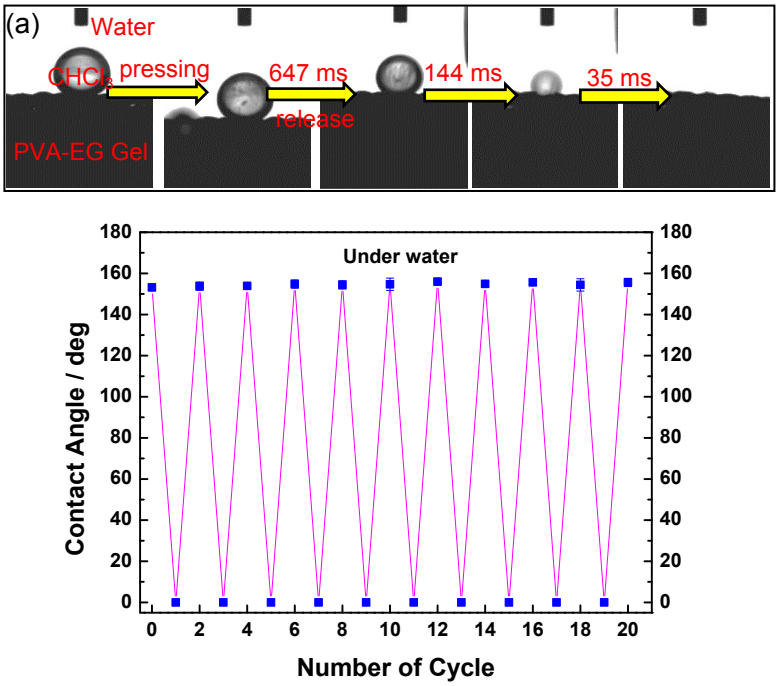


Fig. S11. (a) Underwater contact angles of a $CHCl_3$ droplet on the superhydrophobic integrated PVA-EG/mesh during the pressing/releasing process. (b) Underwater switch of the $CHCl_3$ droplets on the mesh.

In order to switch between superoleophobicity and superoleophilicity in water, the copper mesh without treating with 1H,1H,2H,2H-perfluorodecyltriethoxysilane was used to integrate with superhydrophobic PVA-EG gel. After the integrated PVA-EG/mesh was immersed in water, switch of superoleophobicity/superoleophilicity was carried out by using $CHCl_3$ droplets *via* the pressing/release processes.

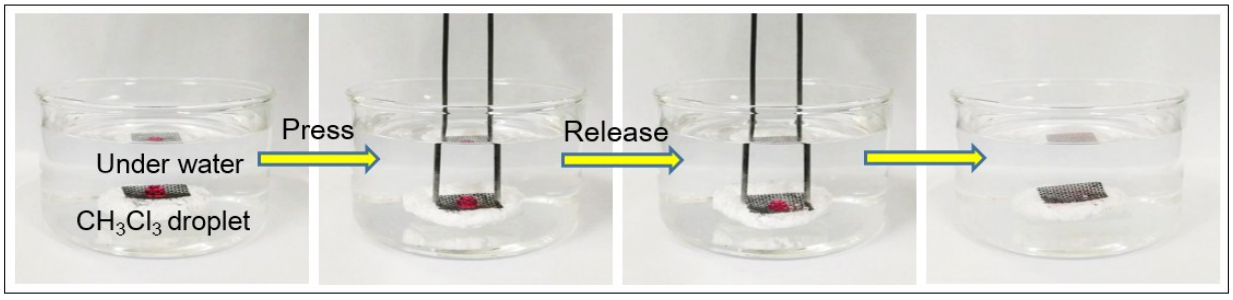


Fig. S12. Optical images show the wettability switch of a $CH_3Cl_3$ droplet on the integrated PVA-EG/mesh in water.

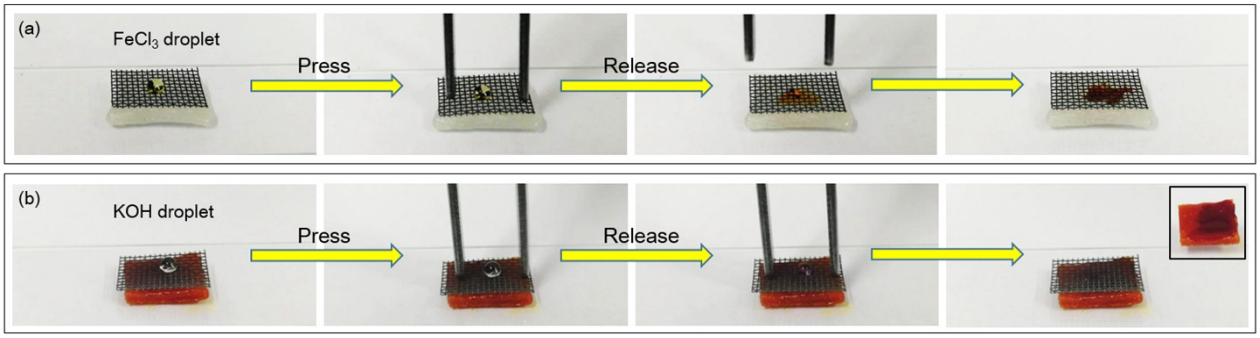


Fig. S13. Identification of microdroplets containing (a) $Fe^{3+}$ and (b) KOH on the integrated superhydrophobic mesh. The underlying gel contained NaSCN (top) and methyl red (bottom).

## References

1 Z. Chu and S. Seeger, *Adv. Mater.*, 2015, **27**, 7775.

2 J. Zhang and S. Seeger, *Adv. Funct. Mater.*, 2011, **21**, 4699.

3 C. L. Cheng and D. Y. Wang, *Angew. Chem. Int. Ed.*, **2016**, *128*, 6967.

4 Q. M. Pan, M. Wang and H. B. Wang, *Appl. Surf. Sci.*, **2008**, *254*, 6002.

5 T. W. Scharf, R. D. Ott, D. Yang and J. A. Barnard, *J. Appl. Phys.*, 1999, **85**, 3142.

6 J. Choi, M. Kawaguchi, T. Kato, *J. Appl. Phys.*, 2002, **91**, 7574.

7 X. Zhang, P. Zhang, Z. Wu and Z. Zhang, *J. Mater. Sci.*, 2012, **47**, 2757.

8 X. Chen, L. Kong, D. Dong, G. Yang, L. Yu, J. Chen and P. Zhang, *Appl. Surf. Sci.*, 2009, **255**, 4015.

9 J. Yu and J. Ran, *Energy Environ. Sci.*, 2011, **4**, 1364.

10 A. B. Gurav, Q. Guo, Y. Tao, T. Mei, Y. Wang and D. Wang, *Mater. Lett.*, 2016, **182**, 106.

11 Z. Dang, L. Liu, Y. Li, Y. Xiang and G. Guo, *ACS Appl. Mater. Interfaces*, 2016, **8**, 31281.

12 P. Raturi, K. Yadav and J. P. Singh, *ACS Appl. Mater. Interfaces*, 2017, **9**, 6007.

13 J. H. Guo, J. K. Wang, Y. H. Gao, J. Wang, W. B. Chang, S. Y. Liao, Z. M. Qian and Y. X. Liu, *ACS Sustainable Chem. Eng.*, 2017, **5**, 10772.

14 H. Zhu, D. Chen, N. Li, Q. Xu, H. Li, J. He and J. Lu, *Adv. Funct. Mater.*, 2015, **25**, 597.

15 S. L. Feng, Y. Xing, S. Y. Deng, W. F. Shang, S. Li, M. X. Zhang, Y. P. Hou and Y. M. Zheng, *Adv. Mater. Interfaces*, 2018, **5**, 1701193.

16 H. Che, M. Huo, L. Peng, T. Fang, N. Liu, L. Feng, Y. Wei and J. Yuan, *Angew. Chem., Int. Ed.*, 2015, **54**, 8934.

17 J. L. Yong, F. Chen, Q. Yang, Y. Fang, J. L. Huo and X. Hou, *Chem. Commun.*, 2015, **51**, 9813.

18 X. Lin, F. Lu, Y. Chen, N. Liu, Y. Cao, L. Xu, W. Zhang and L. Feng, *Chem. Commun.*, 2015, **51**, 16237.

19 W. Sun, S. X. Zhou, B. You and L. M. Wu, *J. Mater. Chem. A*, 2013, **1**, 10646.

20 L. P. Heng, T. Q. Guo, B. Wang, L. Z. Fan and L. Jiang, *J. Mater. Chem. A*, 2015, **3**, 23699.

21 L. Chang, H. Liu, Y. Ding, J. Zhang, L. Li, X. Zhang, M. Liu and L. A. Jiang, *Nanoscale*, 2017, **9**, 5822.

22 H. Liu, X. Zhang, S. Wang and L. Jiang, *Small*, 2015, **11**, 3338.